Molecular determinants of non-competitive antagonist binding to the mouse GPRC6A receptor

Helene Faure[a], Tatiana Gorojankina[a], Nadejda Rice[a], Philippe Dauban[b], Robert H. Dodd[b], Hans Bräuner-Osborne[c], Didier Rognan[d], Martial Ruat[a,*]

[a] CNRS, UPR9040, Institut de Neurobiologie Alfred Fessard-IFR 2118, Signal Transduction and Developmental Neuropharmacology Team, 1 avenue de la Terrasse, F-91198 Gif-sur-Yvette, France
[b] CNRS, Institut de Chimie des Substances Naturelles-UPR2301, 1 avenue de la Terrasse, F-91198 Gif-sur-Yvette, France
[c] Department of Medicinal Chemistry, Faculty of Pharmaceutical Sciences, University of Copenhagen, Universitetsparken 2, 2100 Copenhagen, Denmark
[d] CNRS, Institut Gilbert Laustriat, Bioinformatics of the Drug, UMR7175-LC1, F-67400 Illkirch, France

ARTICLE INFO

ABSTRACT

GPRC6A displays high sequence homology to the Ca^{2+}-sensing receptor (CaSR). Here we report that the calcimimetic Calindol and the calcilytic NPS2143 antagonize increases in inositol phosphate elicited by L-ornithine-induced activation of mouse GPRC6A after transient coexpression with $G\alpha_{qG66D}$ in HEK293 cells. The calcilytic Calhex 231 did not modulate this response. A three-dimensional model of the GPRC6A seven transmembrane domains (TMs) was constructed. It was used to identify seven residues strictly conserved within the CaSR and GPRC6A allosteric binding pockets, and previously demonstrated to interact with calcilytics or calcimimetics. The mutations $F666A^{3.32}$, $F670A^{3.36}$, $W797A^{6.48}$ caused a loss of L-ornithine ability to activate GPRC6A mutants. The $F800A^{6.51}$ mutant was not implicated in either Calindol or NPS 2143 recognition. The $E816Q^{7.39}$ mutation led to a loss of Calindol antagonist activity but was without effect on NPS2143 inhibitory response. In summary, these data suggest that Calindol is primarily anchored through an H-bond to $E816^{7.39}$ in TM7 and highlight important local differences at the level of the CaSR and GPRC6A allosteric binding pockets. We have identified the first antagonists of GPRC6A that could represent new tools to analyze GPRC6A functions and serve as chemical leads for the development of more specific modulators.

© 2009 Elsevier Ltd. All rights reserved.

1. Introduction

Among G-protein coupled receptors (GPCRs), those of family 3 have recently been the focus of intense studies for the discovery of allosteric modulators binding to the transmembrane domains (TMs) [1]. This family includes 8 metabotropic receptors (mGluR1–8), 2 γ-aminobutyric acid type B receptors, 3 taste receptors, the calcium sensing receptor (CaSR), the GPRC6A for basic L-α-amino acids and seven orphan receptors [2]. These receptors display several key features including a long bilobed amino-terminal tail containing the orthosteric binding site and a cysteine-rich region connected to a hydrophobic domain formed by 7 putative transmembrane segments. Binding of the ligand to the orthosteric binding site is believed to induce structural changes within the seven TMs allowing signal transmission to occur. Molecules binding to the allosteric site of the mGluRs have

been identified and their therapeutic interest is being evaluated [3]. In the case of the CaSR, intense studies have led to the discovery of allosteric modulators acting at the level of the TMs. Positive allosteric modulators such as Calindol and NPS R-568 and its derivative Cinacalcet, recently introduced clinically for treating disorders linked to chronic renal insufficiency, potentiate the effect of Ca^{2+} [4,5]. Negative allosteric modulators such as Calhex 231 or NPS 2143 which has been shown to inhibit the parathyroid receptor *in vivo* [6], block the effect of Ca^{2+}. These molecules bind to the TMs of the CaSR far away from the Ca^{2+} orthosteric binding site [7]. Preliminary studies indicated that the ligand binding pockets for positive and negative allosteric modulators are overlapping but not identical and identified subtle differences within the binding of the negative allosteric modulators [8–10].

Recently, it has been shown that NPS R-568, a selective and potent CaSR agonist, was also a positive allosteric modulator of the mGPRC6A [11]. These data suggested that other CaSR allosteric ligands might modulate mGPRC6A activation. The CaSR controls calcium homeostasis through the regulation of parathyroid hormone and calcitonin secretion but the functions of the receptor in tissues such as the kidney, the gastrointestinal tract,

* Corresponding author. Tel.: +33 1 69 82 36 41; fax: +33 1 69 82 36 39.
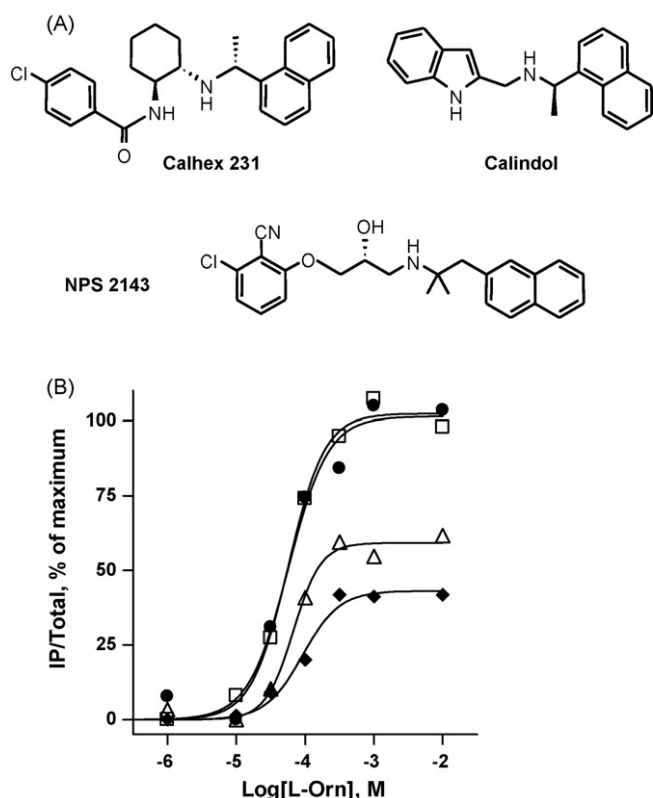E-mail address: ruat@nbcm.cnrs-gif.fr (M. Ruat).

(A)

Calhex 231

Calindol

NPS 2143

(B)

Fig. 1. Effect of calcimimetic and calcilytics on L-Orn-stimulated increase of IP in HEK293 cells coexpressing mGPRC6A and $G\alpha_{qG66D}$.
(A) Chemical structure of Calcilytics:Calhex 231, (1S,2S,1′R)-N[1]-(4-chlorobenzoyl)-N[2]-[1-(1-naphthyl)ethyl]-1,2-diaminocyclohexane; NPS 2143, N-[(R)-2-hydroxy-3-(2-cyano-3-chlorophenoxy) propyl]-1,1-dimethyl-2-(2-naphthyl)-ethyl-amine and Calcimimetic:Calindol(R)-2-[1-(1-naphthyl) ethylaminomethyl]-1H-indole. (B) Inhibition of L-Orn-stimulated increase of IP response by Calindol, NPS 2143 and Calhex 231 in HEK293 cells transiently co-transfected with mGPRC6A and $G\alpha_{qG66D}$. After prelabeling and washing procedures, cells were incubated with increasing concentrations of L-Orn alone (□) or in presence of 10 μM of Calindol (♦), NPS 2143 (△) or Calhex 231 (●) for 30 min. Data are expressed as % of maximal IP response observed with 10 mM L-Orn which represented between 3 and 4 times the IP basal level and are average of duplicates from a typical experiment representative of 3–5 experiments.

bone cells and the brain where its expression has been reported are not well characterized [3–5,12]. The mGPRC6A receptor has been recently identified as a promiscuous L-α-amino acid sensor [13–15]. However, the functional roles of this receptor during embryonic development and in adult tissues are not well understood [16]. Generation of GPRC6A null mice has not allowed to delineate its physiological roles [17,18]. To further understand the evolutionary link between the CaSR and the mGPRC6A within family 3 of GPRCRs, we have evaluated the pharmacological properties with respect to the mGPRC6A of three allosteric modulators of the CaSR with different chemical structures (Calindol, NPS 2143 and Calhex 231; Fig. 1A). We used site-directed mutagenesis of amino acid residues putatively delineating the allosteric binding pocket of the mGPRC6A to analyze the biochemical and pharmacological properties of this receptor.

2. Materials and methods

2.1. Compounds

Calindol(R)-2-[1-(1-naphthyl)ethylaminomethyl]-1H-indole, Calhex 231, (1S,2S,1′R)-N[1]-(4-chlorobenzoyl)-N[2]-[1-(1-naphthyl) ethyl]-1,2-diaminocyclohexane and NPS 2143, N-[(R)-2-hydroxy-

3-(2-cyano-3-chlorophenoxy)propyl]-1,1-dimethyl-2-(2-napht-hyl)ethylamine, were from R.H. Dodd (Gif/Yvette, France), L-ornithine mono chloride (L-Orn) was from Sigma.

2.2. Plasmids

The wild-type (WT) mGPRC6A cDNA in pCR2.1 vector was from Prof. H. Bräuner-Osborne (Copenhagen, Denmark). To generate the Myc-mGPRC6A construct, a fragment encoding amino acid residues 21–928 was amplified by PCR. The restriction fragment MluI–SalI was subcloned in pRK5-SP-myc vector [19]. pcDNA3 plasmid containing the N-terminal myc-tagged human CaSR (hCaSR) was kindly provided by Prof. G.N. Hendy (Montreal, Canada) and was previously described [20]. $G\alpha_{qG66D}$-containing plasmid was a kind gift of Dr. E. Kostenis (Bonn, Germany) and was described previously [21].

2.3. Site-directed mutagenesis

All point mutations in mGPRC6A and hCaSR were introduced using the QuikChange site-directed mutagenesis kit (Stratagene) with specific oligonucleotides (Eurobio, Les Ulis, France). All final constructions were verified by sequencing on both strands (Genome Express, Meylan, France). Oligonucleotide sequences are available upon request.

2.4. Cell culture and transfections

HEK293 cells (Eurobio, Les Ulis, France) were cultured in Dulbecco's modified Eagle's medium supplemented with 10% fetal calf serum (Invitrogen) and were transiently transfected with plasmid containing WT or mutant hCaSR by electroporation as described [10]. In the case of WT or mutated mGPRC6A, 4 μg were supplemented with $G\alpha_{qG66D}$ (4 μg) and pRK5 empty vector (2 μg) [19]. After electroporation, cells were resuspended in culture medium and distributed on a 6-well plate for Western blot analysis or on a 24-well plate coated with poly-D-lysine (0.05 mg/ml, Sigma) for measurement of [3H]inositol phosphates ([3H]IP) formation. 48 h after transfection cells were used for analysis. Alternatively, the cells were resuspended in 13 ml of culture medium, then distributed (200 μl) on white 96-well plates (VWR) coated with poly-D-lysine (0.05 mg/ml) and used to measure inositol phosphate production using IP-One HTRF assay 48 h later.

2.5. [3H]IP formation

Cells were labeled with 0.5 μCi/well of myo-[3H]inositol (GE Healthcare) for 20 h in their growth medium. Measurement of [3H]IP accumulation for WT and E837 mutant hCaSR was performed as described [10]. Their activities were determined in response to increasing extracellular Ca^{2+} or to NPS 2143 in the presence of 9 mM Ca^{2+}. For measurement of WT and mutant mGPRC6A activities, cells were washed and preincubated 2× 2 h at 37 °C in HBSS buffer (pH 7.4) containing 3.5 mM $NaHCO_3$, 20 mM HEPES, 1 mM $CaCl_2$ and 1 mg/ml bovine serum albumin. The activities of WT and mutant mGPRC6A were then determined in response to increasing concentration of L-Orn alone or in the presence of NPS 2143, Calhex 231 or Calindol (10 μM) and 2 mM Ca^{2+} as described [10,22]. Data are expressed as the average of duplicate determinations and are representative of 3–8 independent experiments. IC_{50} for NPS 2143 on hCaSR and EC_{50} values for L-Orn were calculated using GraphPad Prism 2.01 (GraphPad Prism Software Inc., San Diego, CA). Significance was assayed by the Excel 98 Student's t-test (Microsoft, Seattle, WA).

2.6. HTRF IP-One assay

HTRF experiments were performed following IP-One bulk kit (Cisbio, France) instructions with the following adaptations. 48 h after transfection HEK293 cells were washed and preincubated $2\times$ 2 h at 37 °C in 100 μl of HBSS buffer (as for measurement of [3H]IP formation). The buffer was then replaced with 70 μl of stimulation buffer containing the indicated L-Orn and drug concentrations and 2 mM Ca^{2+}. After 30 min incubation at 37 °C, the reaction was stopped. Assay plates were then incubated for 1 h at room temperature. FRET and fluorescence signals were measured 50 μs after excitation at 337 nm, at 620 and 665 nm, using a Genios Pro apparatus (TECAN, Austria GmbH). The assay signal was expressed as the HTRF ratio [(fluorescence at 665 nm/fluorescence at 620 nm) $\times 10^4$] and converted to nM of IP1 using an IP1 calibration curve.

2.7. Western blot analysis

Cell lysates and Western blots were performed as previously described [10]. Nitrocellulose membranes were probed for 2 h at room temperature with 9E10 (1:400), a mouse monoclonal anti-Myc antibody (Sigma). A horseradish peroxidase conjugated goat anti-mouse IgG was used as secondary antibody (Chemicon International). The immunoreactivity was revealed with enhanced chemiluminescence kit ECL (GE Healthcare).

2.8. Immunocytochemistry

The immunofluorescence experiments were performed essentially as described [23]. For Calindol pretreatment experiments, 24 h after transfection Calindol was added into the media to a final concentration of 20 μM. Equal amount of vehicle was added to control cells and incubation continued overnight. For the detection of the protein at the cell surface, cells were incubated for 90 min at 37 °C in the culture medium without serum with 9E10 (1:400) monoclonal antibody and then fixed in 4% paraformaldehyde. For the detection of the protein inside and at the cell surface, cells were first fixed in 4% paraformaldehyde, then permeabilized with 0.05% Triton X-100 and incubated for 2 h at RT in PBS–2% gelatin supplemented with 9E10 (1:400). A 1:1000 dilution of FITC-labeled goat anti-mouse IgG (Sigma) was used as secondary antibody and Vectashield medium as mounting medium (AbCys, Paris, France). The immunofluorescence staining was visualized and analyzed under a Leica fluorescence microscope. Negative controls were performed in parallel on mock-transfected cells.

2.9. Residue numbering and nomenclature

The Ballesteros–Weinstein residue numbering scheme [24] was used throughout for GPCR TMs helices. For application to the second extracellular loop (ECL2), corresponding residues have been labeled 45.x, 45 indicating the location between TMs 4 and 5 (therefore ECL2) and x a number relative to the conserved cysteine residue which is assigned number 50. Numbers lower than 50 thus describe upstream residues located between TM4 and C45.50. Numbers higher than 50 describe downstream residues located between C45.50 and TM5. For explicit numbering of residues in specific receptors, the UniProt [25] residue number is given before the Ballesteros number in superscript (e.g. E816[7.39] for mGPRC6A).

2.10. Three-dimensional model of the mouse GPRC6A and of the allosteric binding pocket

A model of the mGPRC6A TMs (residues 588–835) was derived from our previously published model of the hCaSR [10]. Both sequences (mGPRC6A: D588-K685; hCaSR: S607-K856) were aligned using standard settings of the ClustalW2 algorithm [26]. hCaSR residues were mutated to mGPRC6A residues using the Biopolymer module of the Sybyl 8.0 package (TRIPOS Assoc., Inc., St-Louis, USA) keeping dihedral angle values of the mutated side chains. Since no major insertion/deletion could be noticed, hydrogen atoms could be added using standard geometries in SYBYL. Starting coordinates were then embedded in a 10-Å wide water box (TIP3P model) in Amber 8.0 (University of California, San Francisco, CA 94158-2517, USA) and further refined with the ff03 force-field [27] by 2000 steps of steepest-descent followed by 3000 steps of conjugate-gradient energy-minimization.

2.11. Automated docking of NPS 2143 and Calindol

NPS 2143 and Calindol input three-dimensional structures were obtained by converting 2D Marvin sketches (ChemAxon Ltd., Budapest, Hungary) into three-dimensional mol2 files with Corina v3.4 (Molecular Networks, Erlangen, Germany). Both compounds were docked with Gold v4.0 docking program into a cavity delimited by 30 residues featuring a canonical ligand binding site of most if not all GPCRs [28] to which were added 5 amino acids encompassing the conserved cysteine residue in the second extracellular loop (L742-E746). Automated settings of the Gold genetic algorithm were chosen in order to scale parameters according to ligand flexibility. A maximum of 30 poses were saved for each ligand and the diversity of obtained binding modes was analyzed by computing molecular interaction fingerprints with the receptor model using the in-house developed IFP program [29].

3. Results

3.1. Calindol and NPS 2143 but not Calhex 231 are non-competitive antagonists of mGPRC6A

We have shown previously that Calhex 231 and NPS 2143 are negative allosteric modulators of the CaSR whereas Calindol and NPS R-568 act as positive allosteric modulators [9,10,30,31]. Recently, Pi et al. [11] have reported that NPS R-568 (0.5 μM) stimulated SRE promoter-luciferase reporter activity in HEK293 cells after transfection of a Myc epitope tagged GPRC6A cDNA. This observation prompted us to analyze the effect of Calhex 231, NPS 2143 and Calindol at the mGPRC6A. First, we developed a functional assay for mGPRC6A based on a method previously published by Christiansen et al. [13]. We transiently co-transfected mGPRC6A and the promiscuous $G\alpha_{qG66D}$ protein in HEK293 cells and monitored IP formation upon stimulation with L-Orn. Increasing the concentration of L-Orn from 1 μM to 1 mM caused a 3–4-fold increase of IP accumulation measured using an HTRF (IP-One) or a radioactive ([3H]IP) assay, respectively (Suppl. Fig. 1). We did not detect an increase of IP accumulation in HEK293 cells transiently transfected solely with an empty plasmid, a plasmid containing the mGPRC6A or the $G\alpha_{qG66D}$ after addition of 10 mM L-Orn (data not shown). Analysis of the L-Orn dose–response curves led to an EC_{50} for L-Orn of 44 ± 6 μM (mean ± S.E.M., $n = 6$) and 64 ± 5 μM (mean ± S.E.M., $n = 9$) using the HTRF or the radioactive assay, respectively (Tables 1 and 2). These data fit well with the affinity for L-Orn determined in an IP turnover assay at the mGPRC6A expressed in tsA201 cells [13].

Next, we evaluated the effects of Calhex 231, Calindol and NPS 2143 by analyzing the concentration–response curves for stimulation of IP formation in response to L-Orn in the absence or in the presence of 10 μM of these compounds. Incubation of HEK293 cells coexpressing mGPRC6A and $G\alpha_{qG66D}$ with Calindol or NPS 2143 caused a marked and significant reduction in the amplitude of the IP response as compared with the stimulation evoked with L-Orn

Table 1
Summary of the effects of various mGPRC6A mutations.

Receptor	Position	Cellular localization	Maximal response (% of WT)	L-Orn EC$_{50}$ (μM)
WT		M	100 ± 5	44 ± 6
R662A	TM3	IC	<20	ND
F666A	TM3	M*	<20	ND
F670A	TM3	M	<20	ND
W797A	TM6	M	44 ± 10	>300
F800A	TM6	M	103 ± 10	22 ± 6
E816A	TM7	IC	<20	ND
E816Q	TM7	M	87 ± 1	28 ± 15
E816D	TM7	IC	<20	ND
E816L	TM7	IC	<20	ND
I820A	TM7	IC	<20	ND

Cellular localization of the WT and the different mutant mGPRC6As assessed from immunocytochemistry. Concentration–response curves for L-Orn were generated as described in legends to Figs. 3 and 4. EC$_{50}$ values and maximal stimulation for L-Orn (at 10 mM) were compared with the maximal L-Orn response of the WT mGPRC6A. Data shown are means $\pm$ S.E.M. from 3 to 10 independent experiments. M: presence at the cell membrane, IC: intracellular, ND: not determined, *weak expression.

Table 2
Summary of the functional effects of F800A and E816Q mutations of mGPRC6A.

Receptor	L-Orn EC$_{50}$ (μM)				Maximal response (%)			
	Control	NPS 2143	Calindol	Calhex 231	Control	NPS 2143	Calindol	Calhex 231
WT	64 ± 5	62 ± 3	67 ± 19	61 ± 14	100	$61 \pm 7^*$	$49 \pm 7^*$	103 ± 1
F800A	27 ± 3	30 ± 3	64 ± 10	ND	100	$59 \pm 9^*$	$34 \pm 3^*$	ND
E816Q	89 ± 6	63 ± 3	63 ± 7	ND	100	$62 \pm 5^*$	94 ± 3	ND

Concentration–response curves for L-Orn alone (control) or in the presence of 10 μM NPS 2143, Calindol or Calhex 231 were generated as described in the legends of Figs. 1 and 5. Maximal response to 10 mM L-Orn alone (taken as 100%) or in the presence of NPS 2143, Calindol or Calhex 231 was compared for each receptor. Level of significance: $^*p < 0.001$ compared with the control for each receptor.

alone whereas Calhex 231 did not (Fig. 1B and Table 2). Interestingly, despite the profound reduction of the response amplitude, the EC$_{50}$ values of L-Orn were not affected. These observations indicate that Calhex 231 is not an antagonist of mGPRC6A whereas both Calindol and NPS 2143 are non-competitive antagonists of L-Orn binding to the mGPRC6A.

mGPRC6A and hCaSR display a high sequence homology not only throughout the extracellular domain but even more along the seven TMs. Based on a previously described model of hCaSR [10], we have now developed a model of mGPRC6A and used it to define a putative ligand binding site for allosteric modulators such as those identified for the CaSR and other family 3 GPCRs [10,28]. Thus, 33 mGPRC6A residues involved in this putative binding pocket were compared to those shown to delineate the hCaSR binding pocket (Fig. 2). 18 residues were identical and several others were conserved. Interestingly, 7 residues located in TM3, TM6 and TM7 previously demonstrated by site-directed mutagenesis to participate in calcilytic (NPS 2143 and Calhex 231) recognition by the hCaSR were identical. Among them, W$^{6.48}$, F$^{6.51}$, E$^{7.39}$ and I$^{7.43}$ have also been shown to participate in Calindol binding. These observations suggest that NPS 2143 and Calindol may bind to mGPRC6A TMs through interaction with these residues.

3.2. Generation of point mutations and characterization of the mutant mGPRC6A receptors

We have mutated the 7 amino acids described above into alanine (see Fig. 2) by site-directed mutagenesis to investigate their possible interaction with NPS 2143 and Calindol. These mutants and the WT mGPRC6A were transiently transfected into HEK293 cells. We then analyzed their ability to respond to L-Orn by measuring the accumulation of IPs, their expression by Western blotting and their subcellular distribution using a Myc antibody which recognizes the Myc epitope located at the amino-terminal tail of the WT and mutant receptors.

We first analyzed mGPRC6A immunoreactivity by microscopy using anti-Myc antibodies on permeabilized and non-permeabilized HEK293 transfected with the WT and the various mutant constructs. Myc immunoreactivity was detected at the cell surface of non-permeabilized HEK293 cells transfected with WT mGPRC6A (Fig. 3A). After cell permeabilization, immunoreactivity was also observed at the cytoplasmic level. In cells transfected with the empty vector, Myc immunoreactivity was not detectable under either condition (data not shown). These data suggest that mGPRC6A is addressed to the cell membrane. Under reducing SDS PAGE conditions, three polypeptides migrating with a mobility corresponding to molecular masses of 115, 105 and 80 kDa were identified in whole lysates from cells transfected with the WT receptor. These signals were absent in mock-transfected cell preparations thereby indicating their specificity. A polypeptide complex migrating above 200 kDa was also observed and likely correspond to intermolecular linked dimers of the receptor as previously observed (Fig. 3B) [32]. The 115 kDa peptide might correspond to glycosylated receptors whereas the 105 kDa peptide is consistent with the molecular weight of the unglycosylated receptor as previously reported for the rat and mouse GPRC6A [14,32] whereas the 80 kDa peptide presumably represents a proteolytic. Importantly, the expression pattern of the various mutant receptors was almost comparable to that of the WT receptor as accessed by immunoblotting (Fig. 3B) except for the
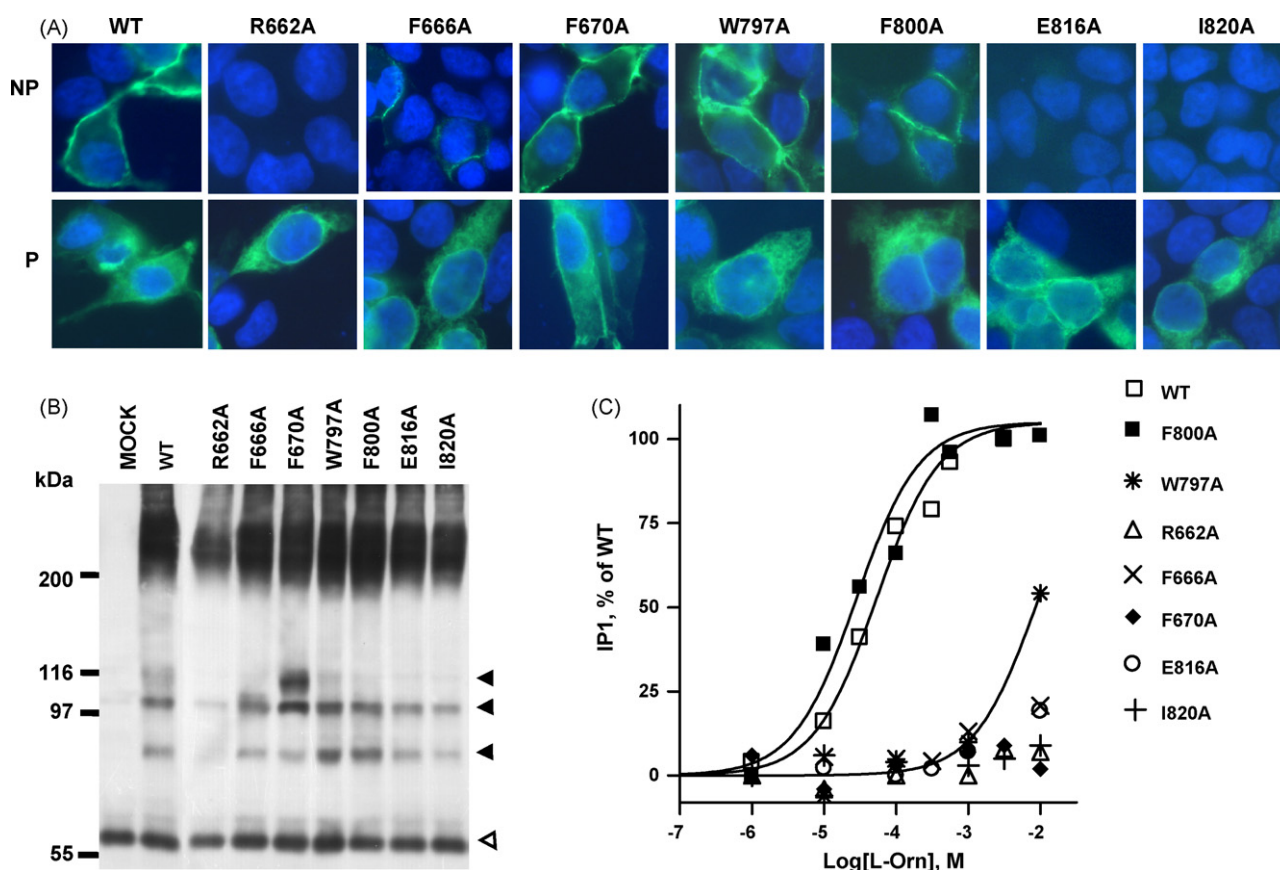


```
                1.35
                1.39
                1.42
                1.46
                1.57
                2.58
                2.61
                2.65
                3.28
                3.32
                3.36
                4.56
                4.60
                45.49
                45.51
                45.52
                5.38
                5.42
                5.43
                5.46
                6.48
                6.51
                6.52
                6.55
                7.39
                7.43
                7.45
hCASR:    FLFGCFSIRQFGFIYPTHEALLITFWFIYVEIA
mGPRC6A:  LLLGNFTIRQFGFVVPEEEAFMLIYWFIYLEII
                      *  *  *        **      **
```

Fig. 2. Comparison of 33 amino acid residues delineating the TMs cavity of the mGPRC6A and hCaSR.
Identical residues are in grey. Residues that have been implicated in calcilytic (NPS 2143 and Calhex 231) or calcimimetic (Calindol) binding in hCaSR and assayed by site-directed mutagenesis in mGPRC6A are indicated by stars. Numbers indicate amino acid position (Ballesteros numbering) within the putative transmembrane domains.

Fig. 3. Functional analysis of the WT and mutant mGPRC6As.
(A) Analysis of mGPRC6A expression by immunocytofluorescence in HEK293 cells. Cells were transfected with the wild-type (WT) or mutant receptors. The extracellular N-terminal Myc tag was detected using an anti-Myc antibody on non-permeabilized (NP) or permeabilized (P) cells. Protein expression was visualized using a fluorescent secondary antibody detected by conventional microscopy. (B) Immunoblot analysis of whole cell lysates (4 µg proteins) from HEK293 cells transiently transfected with an empty vector (MOCK), or a vector containing the WT or the indicated mGPRC6A mutant, was performed following SDS polyacrylamide gel electrophoresis. mGPRC6A proteins were detected using the anti-Myc antibody 9E10. The position of the molecular mass markers is shown on the left (kDa). Arrow heads (black and white) on the right indicate major bands corresponding to the WT and mutant receptors and to a non-specific band, respectively. (C) Concentration–response curves of L-Orn-induced IP accumulation measured by the IP1 immunoassays in HEK293 cells transfected with WT or mutant receptors and coexpressing $G\alpha_{qG66D}$. The IP response to L-Orn is expressed as % of maximal response to 10 mM L-Orn observed at the WT receptor. Data are means of triplicates from a typical representative experiment out of 3–5.

signal corresponding to the 115 kDa peptide which was stronger in the F670A mutant. By contrast, in non-permeabilized cells, Myc immunoreactivity was detected at the cell membrane of F670A, W797A, F800A mutants and at a low level of F666A, but not R662A, E816A and I820 mutants. After cell permeabilization, immunoreactivity was detected at the cytoplasmic levels in HEK293 cells transfected with each mutant construct.

We then tested the functional activity of the WT and mutant receptors by analyzing their sensitivity to L-Orn. Among all tested mutants, only F800A displayed a dose–response curve to L-Orn comparable to the WT receptor (Fig. 3C and Table 1). All other tested mutants did not give a significant activity in response to L-Orn except the W797A mutant which showed a significant and reproducible increase in the IP response to elevated L-Orn concentration (up to 10 mM). Together with the expression and distribution profile of these proteins, these data suggest that the mGPRC6A proteins harboring the F666A, F670A, or W797A mutations are targeted to the cell membrane but have lost all or most of their sensitivity to L-Orn whereas the R662A, the E816A and I820A mutants are trapped inside the cell. In agreement, these last mutants, when transfected in HEK293 cells, did not lead to IP accumulation in response to L-Orn (10 mM) (Fig. 3 and Table 1). These data demonstrate that the mutation into alanine of 6 residues of the 7 putatively implicated in the recognition of NPS 2143 and Calindol, profoundly affects either the targeting of the protein or its sensitivity to L-Orn.

3.3. Calindol binding requires the E816 residue located in TM7 of mGPRC6A

We have previously shown that the residue E837[7.39] plays a key role in both Calindol and NPS 2143 recognition in the hCaSR [9]. Here, the corresponding E816A[7.39] mGPRC6A mutant was trapped inside the cell which did not allow us to analyze its pharmacological properties. These data suggest that this mutation affects the three-dimensional structure of the receptor in such a way that it dramatically modifies its targeting to the cell membrane. We decided to mutate the E816[7.39] residue into an aspartate, a glutamine or a leucine residue and to analyze the expression and the functional properties of the associated mutants in HEK293 cells. The aspartic acid and leucine substitution led to mutants that were also trapped inside the cell (Fig. 4A) whereas the glutamine mutant was well expressed at the cell membrane. Since the expression of these mutants was comparable to the expression of the WT receptor as judged by Western blot analysis of transfected cells, these data suggest that a slight variation in the length of the side chain (shorter in the case of aspartic acid and alanine) or its hindrance (in the case of leucine) disrupted the ternary structure of the mutant receptor affecting the targeting of the protein. However, a change of the acidic residue into the corresponding neutral amino acid did not lead to an apparent change in the distribution of the mutant receptor at the cell membrane. When these mutants were tested in
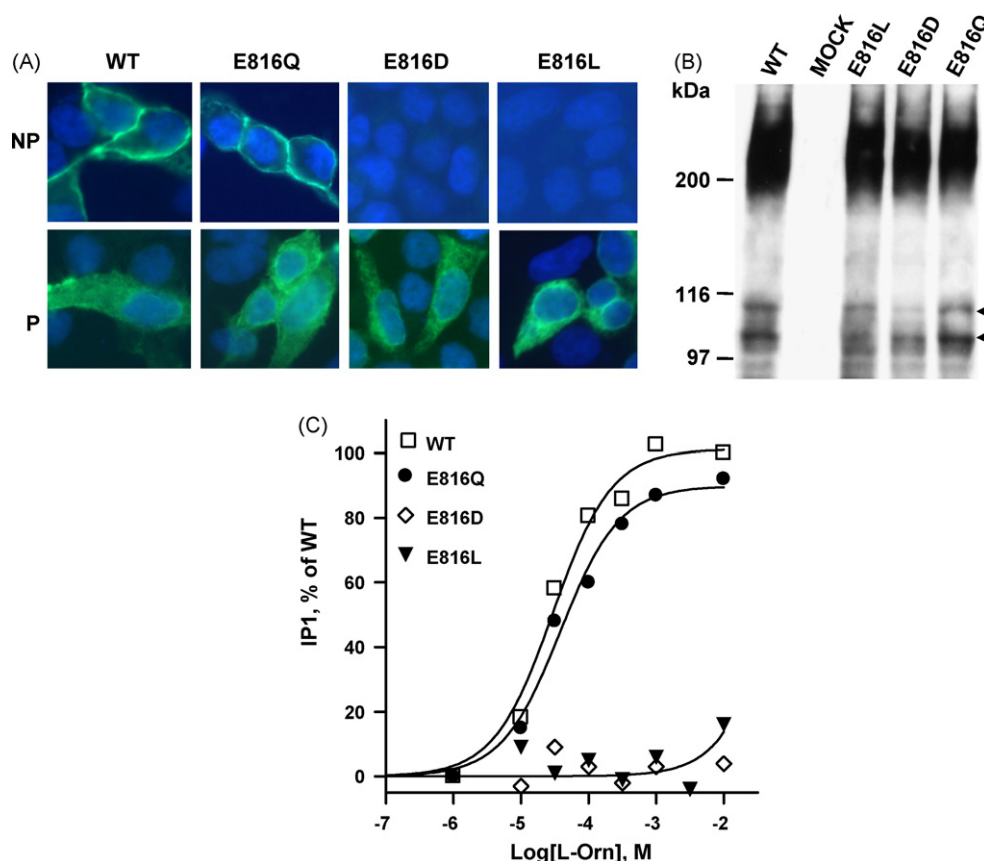
Fig. 4. Functional effect of mutations affecting the E816 mGPRC6A residue.
HEK293 cells were transfected with the mock plasmid or with a plasmid encoding the WT, the E816Q, the E816D, or E816L mGPRC6A mutants. Analysis of mGPRC6A expression by immunocytofluorescence (non-permeabilized (NP) or permeabilized (P) cells) (A) and Western blot (B) were performed as described in the legend of Fig. 3A and B. (B) The position of the molecular mass markers is shown on the left. Arrow heads on the right indicate the molecular weight of two major bands corresponding to mGPRC6A. (C) Concentration–response curves to L-Orn measured by the IP-One assay as described in Fig. 3C. Data are means of triplicates from a typical representative experiment out of 3–5.

IP assays, the E816Q mutant displayed a dose–response curve to L-Orn comparable to the WT receptor whereas the E816D and E816L mutants were inactive, in agreement with their lack of expression at the cell membrane (Fig. 4A, C and Table 1).

We then tested the ability of NPS 2143 and Calindol to inhibit the IP response induced by L-Orn in HEK293 cells transfected with the F800A and E816Q mutants (Fig. 5A and B). Both Calindol and NPS 2143 (10 μM) reduced the IP response induced by L-Orn on the F800A mutant. Again, we observed a marked reduction of the maximal response without a modification of its EC_{50} suggesting that both compounds behaved as non-competitive antagonists. These data clearly indicate that the F800 residue does not interact with either antagonist. Interestingly, in HEK293 cells transfected with the E816Q mutant, the IP response to L-Orn was not modified by Calindol (10 μM) whereas the maximal response was diminished by NPS 2143 (10 μM) (Fig. 5B). These data suggest that the E816 residue is implicated in the recognition of Calindol but not of NPS 2143, which either indicates that recognition of NPS 2143 by mGPRC6A does not require the E816 residue or that the hydroxyl and amine function of NPS 2143 are still H-bonded to Q816.

When the E816D mutant was transiently expressed in HEK293 cells and preincubated overnight with Calindol, it was then addressed to the plasma membrane as analyzed by immunoreactivity observed on non-permeabilized cells. Preincubation with the vehicle did not allow modification of the receptor localization (Fig. 5C). These data further suggest that Calindol can bind to E816D mutant allowing further receptor targeting to the cell membrane.

Such interaction was not observed when E816L and E816A mutants were analyzed (Fig. 5C).

To compare the properties of the 7.39 residue from mGPRC6A and the hCaSR, we introduced the E837Q mutation into the hCaSR. This mutant responded well to Ca^{2+} (EC_{50} = 6.3 ± 0.1 mM) and with a maximal effect of Ca^{2+} comparable to that of WT hCaSR (Suppl. Fig. 2 and data not shown). We then established the dose–response curve of NPS 2143 required to block the Ca^{2+}-induced IP response on this mutant. We observed that NPS 2143 inhibited Ca^{2+}-induced IP response of the WT hCaSR with an IC_{50} = 0.4 μM in agreement with our previous data [10] but had no effect on the E837Q mutant (Fig. 6). These data confirm that the E837 residue is implicated in NPS 2143 recognition in the hCaSR and that the 7.39 residue in the hCaSR and mGPRC6A are not strictly equivalent.

3.4. Hypothesized binding mode of Calindol and NPS 2143 to the mGPRC6A

A three-dimensional model of mGPR6CA was built from an earlier experimentally validated model of hCaSR [10]. There are only 4 out of the 33 cavity residues (2.57, 4.56, 45.19 and 45.51) which significantly differ between both receptors. Interestingly, two of them are located in the second extracellular loop and are known as ligand-anchoring residues for many GPCR ligands [33].

Automated docking of NPS 2143 and Calindol to the mGPRC6A model with Gold v4.0 program disclosed a preferred binding mode in which the secondary amine moiety of both compounds
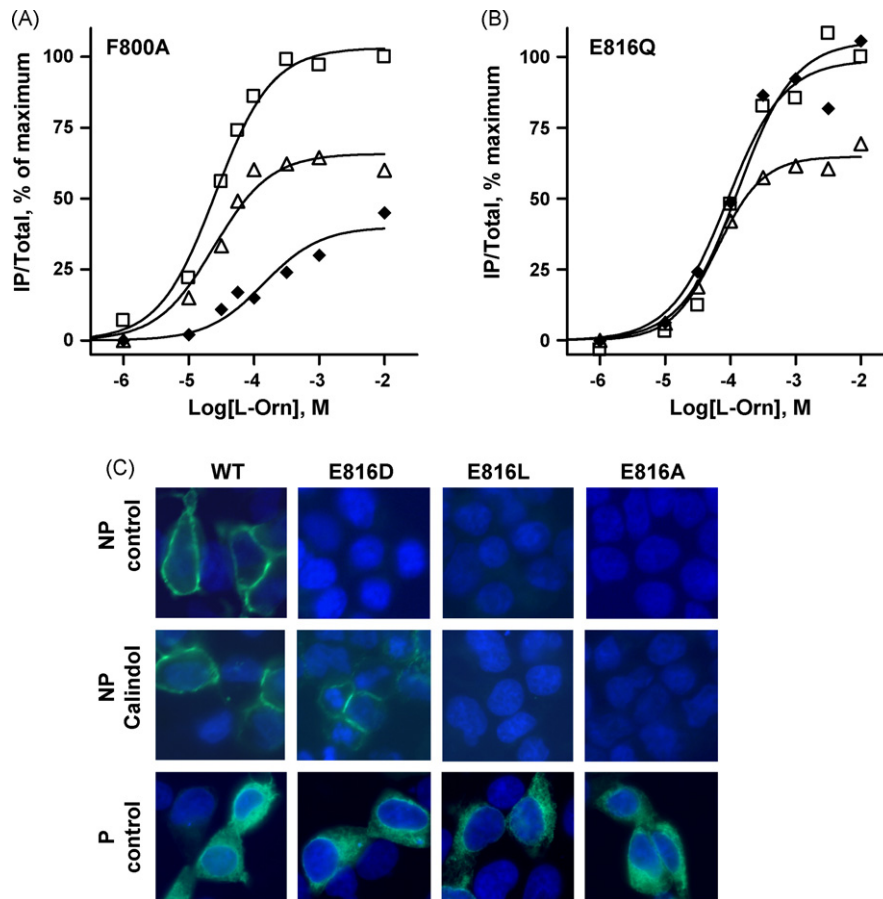
Fig. 5. Effect of Calindol and NPS 2143 on the WT and mGPRC6A E816 and F800 mutants.
(A–B) The cells were transfected with the $G\alpha_{qG66D}$ and the WT, F800A or E816Q mutant vector and the IP response to L-Orn was determined in buffer alone (□) or in the presence of 10 μM Calindol (♦) or NPS 2143 (△). Data are expressed as % of WT receptor response (radioactive assay) to 10 mM L-Orn, which represented 4–8 times the IP basal level. Results are means of triplicates from a representative experiment out of 3–5 ones. (C) Cells were transfected with the WT, or indicated E816 mutant vector. 24 h after transfection, Calindol (20 μM) or control buffer were added to the culture medium and the cells were further incubated overnight. The receptor localization was analyzed by immunocytofluorescence as described in Fig. 3A.
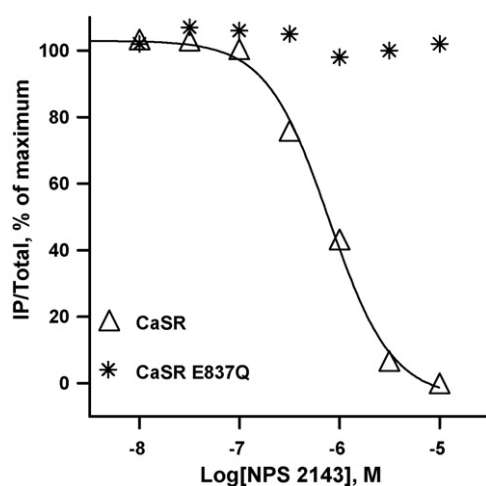

Fig. 6. Effect of NPS 2143 on Ca^{2+}-induced accumulation of IP by the WT and E837Q hCaSR transfected in HEK293 cells.
The cells were transiently transfected with the plasmid encoding the WT or E837Q hCaSR. The IP response induced by 9 mM Ca^{2+} was determined in the presence of increasing concentrations of NPS 2143 for the WT and mutant hCaSR. Data from one experiment out of two are expressed as % of maximal IP response (radioactive assay) observed with 9 mM Ca^{2+} which represented between 4 and 6 times the IP basal level.

is anchored through a salt bridge to the side chain of E816[7.39] (Fig. 7). This main anchoring is further stabilized by an additional hydrogen bond to E816 from the indole nitrogen atom (Calindol) or the secondary alcohol group (NPS 2143). For both ligands, the bound conformation adopts a V-shape conformer in which the two terminal aromatic moieties are embedded in hydrophobic subpockets involving L597[1.39], L600[1.42], F666[3.32], I820[7.43], I822[7.45] on the one side, and F670[3.36], W797[6.48], F800[6.51] and the disulfide bridge C659[3.25]–C744[4.50] on the other (Fig. 7).

4. Discussion

In this study, we have identified Calindol and NPS 2143 as the first two non-competitive antagonists of the mGPRC6A, a member of family 3 GPCRs. These two molecules have been shown to be allosteric modulators of the hCaSR and mediate non-competitive inhibition of L-Orn-induced mGPRC6A activation in cells transiently coexpressing mGPRC6A and $G\alpha_{qG66D}$. Molecular modeling of the TMs region of the mGPRC6A identifies potential amino acid residues delineating a binding pocket for these two molecules. In addition, we have identified E816[7.39] as a key residue involved in Calindol binding to the seven TMs. However, Calhex 231, another chemically different allosteric modulator of the hCaSR, was not active towards modulation of mGPRC6A activation. Altogether, these data demonstrate that the mGPRC6A and hCaSR receptor
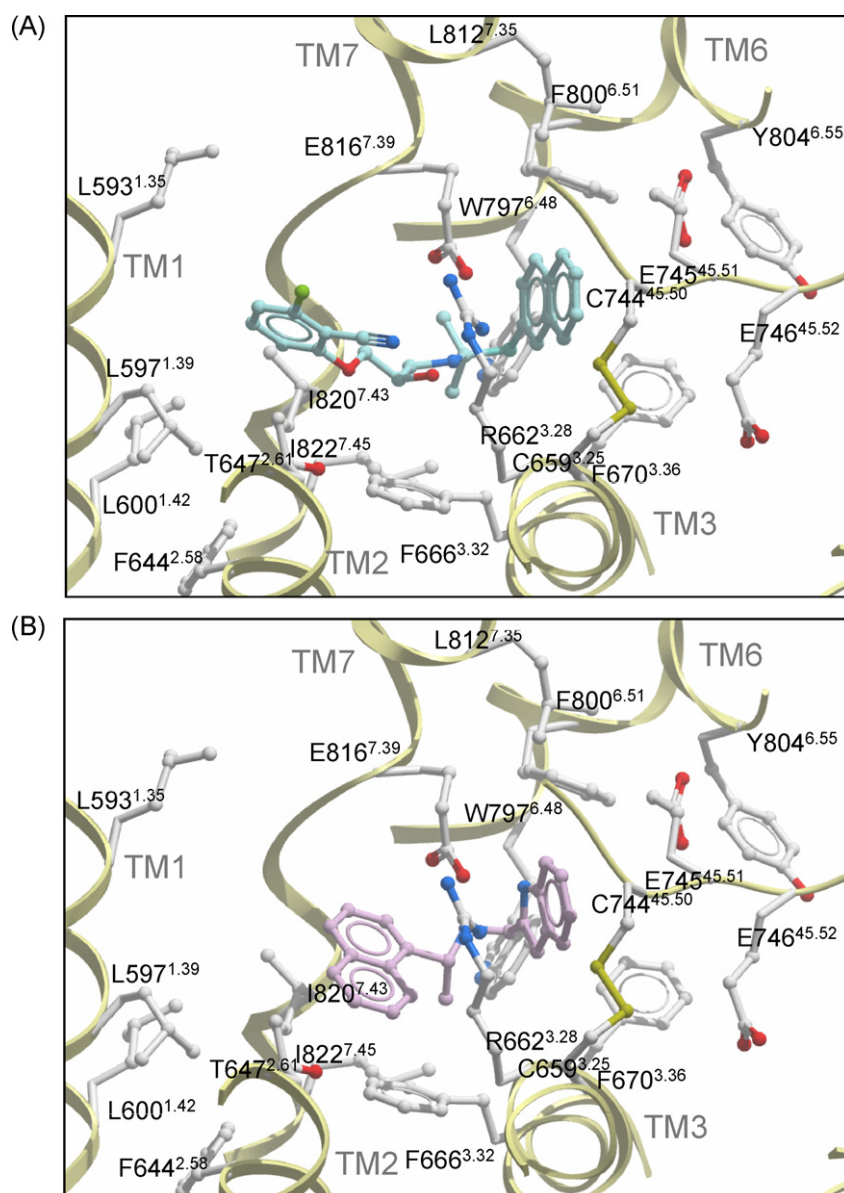
Fig. 7. Proposed models of the mGPRC6A complexed with Calindol and NPS 2143.
Proposed interaction model between NPS 2143 (A), Calindol (B), and the mGPRC6A binding cavity. The seven TMs helices are indicated by yellow ribbons and only important ligand-contacting side chains are displayed as white balls and sticks. Residues are labeled according to the Ballesteros numbering scheme [24]. Three residues (45.50, 45.51, 45.52) of the second extracellular loop which cap the binding site of mGPRC6A allosteric modulators are also displayed. Carbon, oxygen, nitrogen and chlorine atoms are displayed in cyan (NPS 2143) or lavender (Calindol), red, blue and green, respectively.

share similar but not identical ligand binding pockets at the level of the TMs.

The similarities between the mGPRC6A and the hCaSR are evident both through the large extracellular domain (ECD) and the 7 putative TMs that characterize family 3 of GPCRs [34]. However, a striking homology is also observed at the level of the allosteric ligand binding pocket of the mGPRC6A and the CaSR delineated by a set of amino acid residues located within or near the surface of the seven TMs. 18 out of the 33 amino acids lining the seven TMs binding pocket are strictly identical whereas comparison of those involved in the mGPRC6A and mGluR1–8 binding pockets indicates a much lower homology (data not shown). This suggests a putative cross pharmacology between mGPRC6A and hCaSR. The first evidence of this came from the study of Pi et al. [11] which showed that the phenylalkylamine NPS R-568 stimulated SRE-luciferase and ERK activity in HEK293 cells transfected with a GPRC6A plasmid. We noticed that the $E^{7.39}$ residue is present in both the mGPRC6A and CaSR but not in the 2 γ-aminobutyric acid type B receptors, mGluRs or taste receptors. This negatively charged residue participates in the recognition of Calindol, NPS 2143, Calhex 231 and NPS R-568 in CaSR [8–10,35,36] presumably via interaction with the protonated secondary amine present in these molecules. In order to investigate the properties of these molecules towards the mGPRC6A, we developed a Myc-tagged mGPRC6A expressing vector that we co-transfected with $G\alpha_{qG66D}$. mGPRC6A was expressed at the cell membrane and we observed a robust activation of the PLC, as indicated by IP responses, upon stimulation with L-Orn and various amino acids including arginine and arginine derivatives (data not shown) suggesting that mGPRC6A directly interacts with this G-protein in agreement with a previous report [13]. Calindol, NPS 2143 and Calhex 231 on their own did not affect the IP response on mGPRC6A and did not potentiate the IP response induced by 1 μM L-Orn demonstrating that they do not behave as agonists or positive modulators of the mGPRC6A (data not shown). However,

a profound reduction in the amplitude of L-Orn-stimulated IP production was observed in the presence of Calindol and NPS 2143. Since the amplitude change was not accompanied by a modification in the EC_{50} of L-Orn, these data indicated that Calindol and NPS 2143 mediate non-competitive inhibition. These data are in agreement with the presence of the L-Orn binding site within the ECD as previously proposed for these receptors [7,15,37,38] and the location of an allosteric binding site for NPS 2143 and Calindol at the level of the TMs as proposed above.

We have generated a three-dimensional model of the seven TMs of the mGPRC6A that allowed us to identify the putative residues delineating the mGPRC6A allosteric binding pocket. To further test if these residues are implicated in the recognition of NPS 2143 and Calindol, we mutated seven of these residues into alanine and we also submitted the key $E816^{7.39}$ residue to discrete mutations (E816Q, E816D, and E816L). Whereas the mutant receptors were expressed at a level comparable to that of the WT receptor, the R662A, E816A, E816D, E816L and I820A mutants did not reach the cell membrane or only at a low level, were trapped inside the cell and were unsurprisingly not responsive to L-Orn. The receptors harboring the F666A, the F670A and W797A mutations despite being expressed at the cell membrane, were characterized by a decrease of the IP response to L-Orn which was almost completely abrogated in F666A and F670A mutants. Both Calindol and NPS 2143 were able to mediate non-competitive inhibition of L-Orn-induced IP response on the F800A mutant expressed in HEK293 cells, suggesting that this residue does not substantially participate in the binding of these molecules. Interestingly, NPS 2143 but not Calindol was able to inhibit L-Orn-induced stimulation of the PLC in cells expressing the E816Q mutant. However, when the E816D mutant, which was trapped inside the cell, was expressed in HEK293 and preincubated with Calindol overnight, the receptor was then targeted to the cell membrane. This clearly indicated that this mutant receptor still recognizes Calindol. Thus, these data suggest that the protonated secondary amine of Calindol is anchored to the TM7 through an H-bond to the negatively charged E816 residue which is no longer possible in the E816Q mutant, but still possible in the E816D mutant. In the case of NPS 2143, the binding mode remains ambiguous since the hydroxyl moiety of NPS 2143 might still be H-bonded to Q816. Analysis of the CaSR harboring the same mutation at the identical position (E837Q) revealed that the hydroxyl and amine function of NPS 2143 cannot form an H-bond to the Q837 residue. These data demonstrate that despite sharing a similar ligand binding pocket, important differences exist between these two receptors at the level of the allosteric binding site. A significant difference between hCaSR and mGPRC6A binding pockets resides in the nature of residue 45.51 following the conserved cysteine residue implicated in a disulfide bridge in the second extracellular loop. hCaSR presents a histidine at this position whose side chain contributes to one aromatic subpocket accommodating the naphthalene moiety of NPS 2143 [10]. In mGPRC6A, this residue is changed to glutamate (Fig. 2) whose acidic character completely modifies the overall properties of this subpocket and therefore promotes a V-shape bound conformation of the ligand (Fig. 7) and prevents contacts to other aromatic/hydrophobic residues in TMs 5 and 6 (e.g. $Y804^{6.55}$). This particularly bent conformation of both ligands in the GPRC6A binding pocket may explain why the $F800^{6.51}$ mutation to Ala does not affect their binding, by opposition to hCaSR where this residue is predicted to have much more surface contacts with extended conformations of bound ligands [9,10]. Interestingly, the neighboring residue Glu45.52 was also shown to mediate anchoring of JK105, a recently described allosteric regulator of CaSR [39].

It is also worthwhile noting that Calindol behaves as a positive allosteric modulator of the hCaSR and as a negative allosteric modulator of the mGPRC6 which also pinpoints a difference between the two receptors. Site-directed mutagenesis studies on the TMs allosteric site of metabotropic glutamate receptors have already indicated subtle but significant differences in the binding mode of positive and negative allosteric regulators [40] and it has also been demonstrated that closely related ligands can have varying efficacies spanning from negative to positive modulation [40,41].

Negative allosteric modulators of the CaSR have been identified [6,10], and are under intense investigation for the treatment of diseases linked to impaired Ca^{2+} homeostasis. Whereas the positive allosteric modulators presumably facilitate the signal transmitted to the seven TMs by the ECD after binding of the orthosteric ligand, it is thought that the negative allosteric modulators impede this signal. Analysis of the mechanisms of action of these allosteric modulators has revealed novel insights into the receptor activation process suggesting that conformational changes of the seven TMs is crucial for signal transmission [36]. Our data now suggest that mGPRC6A and hCaSR share similarities at the level of the allosteric binding sites for seven TMs modulators but also display important differences. We have published earlier that $E837^{7.39}$ is crucial for Calindol recognition in the CaSR. The present data clearly identify $E816^{7.39}$ to be important for negative allosteric modulation in the mGPRC6A. Therefore, it appears that this residue plays a central role in the activation process of the two receptors but is not able to discriminate by its own whether a molecule will be a positive or a negative modulator.

Like other members of this class of GPCRs, activation of the mGPRC6A is believed to occur upon ligand binding to sites located within the extracellular domain constituted by its long amino-terminal tail [42,43] called a Venus flytrap module [44]. The subsequent conformational change which presumably occurs through the cysteine-rich region affects the seven TMs region leading to receptor activation. Interestingly, several mutations affecting residues located in TM3 and in TM6 of mGPRC6A affect the activation of the receptor by L-Orn. It is possible that these mutations maintain an inactive conformation of the seven TMs region. It is worth noting that the same mutations of these residues in the hCaSR have no or limited effect on Ca^{2+}-mediated receptor activation [9,10] suggesting important differences in the activation process of these two receptors.

Our present data further highlight the complex processes linked to mGPRC6A and CaSR activation and again suggest important differences in these mechanisms. Therefore, further work is needed to understand how allosteric modulators such as NPS 2143 and Calindol can either block direct contact of the VFTM with the seven TMs region of the receptors which functions as a dimer, or can prevent the switch between the inactive and active conformation of the seven TMs region, thus preventing further rotation of TM6 required for activation of many GPCRs [45]. We can thus anticipate that our current model of the hCaSR and mGPRC6A, should facilitate the development of novel positive and negative allosteric modulators displaying improved affinity and selectivity and acting within the seven TMs region of these attractive drug targets. Together with the use of GPRC6A knockout mice [17,18], these molecules should help to further delineate the physiological roles of this receptor.

Acknowledgements

Appendix A. Supplementary data

References

[1] R. Raddatz, H. Schaffhauser, M.J. Marino, Allosteric approaches to the targeting of G-protein-coupled receptors for novel drug discovery: a critical assessment, Biochem. Pharmacol. 74 (2007) 383–391.

[2] M.C. Lagerstrom, H.B. Schioth, Structural diversity of G protein-coupled receptors and significance for drug discovery, Nat. Rev. Drug Discov. 7 (2008) 339–357.

[3] H. Brauner-Osborne, P. Wellendorph, A.A. Jensen, Structure, pharmacology and therapeutic prospects of family C G-protein coupled receptors, Curr. Drug Targets 8 (2007) 169–184.

[4] E.M. Brown, The calcium-sensing receptor: physiology, pathophysiology and CaR-based therapeutics, Subcell. Biochem. 45 (2007) 139–167.

[5] R. Trivedi, A. Mithal, N. Chattopadhyay, Recent updates on the calcium-sensing receptor as a drug target, Curr. Med. Chem. 15 (2008) 178–186.

[6] M. Gowen, G.B. Stroup, R.A. Dodds, et al., Antagonizing the parathyroid calcium receptor stimulates parathyroid hormone secretion and bone formation in osteopenic rats, J. Clin. Invest. 105 (2000) 1595–1604.

[7] C. Silve, C. Petrel, C. Leroy, et al., Delineating a Ca^{2+} binding pocket within the venus flytrap module of the human calcium-sensing receptor, J. Biol. Chem. 280 (2005) 37917–37923.

[8] S.U. Miedlich, L. Gama, K. Seuwen, R.M. Wolf, G.E. Breitwieser, Homology modeling of the transmembrane domain of the human calcium sensing receptor and localization of an allosteric binding site, J. Biol. Chem. 279 (2004) 7254–7263.

[9] C. Petrel, A. Kessler, P. Dauban, et al., Positive and negative allosteric modulators of the Ca^{2+}-sensing receptor interact within overlapping but not identical binding sites in the transmembrane domain, J. Biol. Chem. 279 (2004) 18990–18997.

[10] C. Petrel, A. Kessler, F. Maslah, et al., Modeling and mutagenesis of the binding site of Calhex 231, a novel negative allosteric modulator of the extracellular Ca(2+)-sensing receptor, J. Biol. Chem. 278 (2003) 49487–49494.

[11] M. Pi, P. Faber, G. Ekema, et al., Identification of a novel extracellular cation-sensing G-protein-coupled receptor, J. Biol. Chem. 280 (2005) 40201–40209.

[12] S. Ferry, E. Traiffort, J. Stinnakre, M. Ruat, Developmental and adult expression of rat calcium-sensing receptor transcripts in neurons and oligodendrocytes, Eur. J. Neurosci. 12 (2000) 872–884.

[13] B. Christiansen, K.B. Hansen, P. Wellendorph, H. Brauner-Osborne, Pharmacological characterization of mouse GPRC6A, an L-alpha-amino-acid receptor modulated by divalent cations, Br. J. Pharmacol. 150 (2007) 798–807.

[14] D. Kuang, Y. Yao, J. Lam, R.G. Tsushima, D.R. Hampson, Cloning and characterization of a family C orphan G-protein coupled receptor, J. Neurochem. 93 (2005) 383–391.

[15] P. Wellendorph, K.B. Hansen, A. Balsgaard, et al., Deorphanization of GPRC6A: a promiscuous L-alpha-amino acid receptor with preference for basic amino acids, Mol. Pharmacol. 67 (2005) 589–597.

[16] E. Harno, G. Edwards, A.R. Geraghty, et al., Evidence for the presence of GPRC6A receptors in rat mesenteric arteries, Cell Calcium 44 (2008) 210–219.

[17] M. Pi, L. Chen, M.Z. Huang, et al., GPRC6A null mice exhibit osteopenia, feminization and metabolic syndrome, PLoS ONE 3 (2008) e3858.

[18] P. Wellendorph, L.D. Johansen, A.A. Jensen, et al., No evidence for a bone phenotype in GPRC6A knockout mice under normal physiological conditions, J. Mol. Endocrinol. 42 (2009) 215–223.

[19] C. Masdeu, H. Faure, J. Coulombe, et al., Identification and characterization of Hedgehog modulator properties after functional coupling of Smoothened to G15, Biochem. Biophys. Res. Commun. 349 (2006) 471–479.

[20] L. D'Souza-Li, B. Yang, L. Canaff, et al., Identification and functional characterization of novel calcium-sensing receptor mutations in familial hypocalciuric hypercalcemia and autosomal dominant hypocalcemia, J. Clin. Endocrinol. Metab. 87 (2002) 1309–1318.

[21] A. Heydorn, R.J. Ward, R. Jorgensen, et al., Identification of a novel site within G protein alpha subunits important for specificity of receptor-G protein interaction, Mol. Pharmacol. 66 (2004) 250–259.

[22] M. Ruat, A.M. Snowman, L.D. Hester, S.H. Snyder, Cloned and expressed rat Ca^{2+}-sensing receptor, J. Biol. Chem. 271 (1996) 5972–5975.

[23] J. Coulombe, E. Traiffort, K. Loulier, H. Faure, M. Ruat, Hedgehog interacting protein in the mature brain: membrane-associated and soluble forms, Mol. Cell. Neurosci. 25 (2004) 323–333.

[24] J. Ballesteros, H. Weinstein, Integrated methods for the construction of three-dimensional models and computational probing pf structure–function relations of G protein-coupled receptors, Methods Neurosci. 25 (1995) 366–428.

[25] C.H. Wu, R. Apweiler, A. Bairoch, et al., The Universal Protein Resource (UniProt): an expanding universe of protein information, Nucleic Acids Res. 34 (2006) D187–D191.

[26] M.A. Larkin, G. Blackshields, N.P. Brown, et al., Clustal W and Clustal X version 2.0, Bioinformatics 23 (2007) 2947–2948.

[27] J. Wang, R.M. Wolf, J.W. Caldwell, P.A. Kollman, D.A. Case, Development and testing of a general amber force field, J. Comput. Chem. 25 (2004) 1157–1174.

[28] J.S. Surgand, J. Rodrigo, E. Kellenberger, D. Rognan, A chemogenomic analysis of the transmembrane binding cavity of human G-protein-coupled receptors, Proteins 62 (2006) 509–538.

[29] G. Marcou, D. Rognan, Optimizing fragment and scaffold docking by use of molecular interaction fingerprints, J. Chem. Inf. Model. 47 (2007) 195–207.

[30] A. Kessler, H. Faure, C. Petrel, et al., N1-benzoyl-N2-[1-(1-naphthyl)ethyl]-trans-1,2-diaminocyclohexanes: development of 4-chlorophenylcarboxamide (calhex 231) as a new calcium sensing receptor ligand demonstrating potent calcilytic activity, J. Med. Chem. 49 (2006) 5119–5128.

[31] A. Kessler, H. Faure, C. Petrel, et al., N2-benzoyl-N1-(1-(1-naphthyl)ethyl)-3-phenylpropane-1,2-diamines and conformationally restrained indole analogues: development of calindol as a new calcimimetic acting at the calcium sensing receptor, Bioorg. Med. Chem. Lett. 14 (2004) 3345–3349.

[32] P. Wellendorph, N. Burhenne, B. Christiansen, et al., The rat GPRC6A: cloning and characterization, Gene 396 (2007) 257–267.

[33] C. de Graaf, N. Foata, O. Engkvist, D. Rognan, Molecular modeling of the second extracellular loop of G-protein coupled receptors and its implication on structure-based virtual screening, Proteins 71 (2008) 599–620.

[34] P. Wellendorph, H. Brauner-Osborne, Molecular cloning, expression, and sequence analysis of GPRC6A, a novel family C G-protein-coupled receptor, Gene 335 (2004) 37–46.

[35] J. Hu, G. Reyes-Cruz, W. Chen, K.A. Jacobson, A.M. Spiegel, Identification of acidic residues in the extracellular loops of the seven-transmembrane domain of the human Ca^{2+} receptor critical for response to Ca^{2+} and a positive allosteric modulator, J. Biol. Chem. 277 (2002) 46622–46631.

[36] J. Hu, A.M. Spiegel, Structure and function of the human calcium-sensing receptor: insights from natural and engineered mutations and allosteric modulators, J. Cell. Mol. Med. 11 (2007) 908–922.

[37] H. Brauner-Osborne, A.A. Jensen, P.O. Sheppard, P. O'Hara, P. Krogsgaard-Larsen, The agonist-binding domain of the calcium-sensing receptor is located at the amino-terminal domain, J. Biol. Chem. 274 (1999) 18382–18386.

[38] Y. Huang, Y. Zhou, W. Yang, et al., Identification and dissection of Ca(2+)-binding sites in the extracellular domain of Ca(2+)-sensing receptor, J. Biol. Chem. 282 (2007) 19000–19010.

[39] J. Hu, J. Jiang, S. Costanzi, et al., A missense mutation in the seven-transmembrane domain of the human Ca^{2+} receptor converts a negative allosteric modulator into a positive allosteric modulator, J. Biol. Chem. 281 (2006) 21558–21565.

[40] A. Muhlemann, N.A. Ward, N. Kratochwil, et al., Determination of key amino acids implicated in the actions of allosteric modulation by 3,3′-difluorobenzaldazine on rat mGlu5 receptors, Eur. J. Pharmacol. 529 (2006) 95–104.

[41] J.A. O'Brien, W. Lemaire, T.B. Chen, et al., A family of highly selective allosteric modulators of the metabotropic glutamate receptor subtype 5, Mol. Pharmacol. 64 (2003) 731–740.

[42] E.M. Brown, G. Gamba, D. Riccardi, et al., Cloning and characterization of an extracellular Ca(2+)-sensing receptor from bovine parathyroid, Nature 366 (1993) 575–580.

[43] M. Ruat, M.E. Molliver, A.M. Snowman, S.H. Snyder, Calcium sensing receptor: molecular cloning in rat and localization to nerve terminals, Proc. Natl. Acad. Sci. U.S.A. 92 (1995) 3161–3165.

[44] N. Kunishima, Y. Shimada, Y. Tsuji, et al., Structural basis of glutamate recognition by a dimeric metabotropic glutamate receptor, Nature 407 (2000) 971–977.

[45] H. Schwalbe, G. Wess, Dissecting G-protein-coupled receptors: structure, function, and ligand interaction, Chembiochem 3 (2002) 915–919.